Multi-biomarker pharmacokinetic-pharmacodynamic relationships of central nervous systems active dopaminergic drugs

Brink, W.J. van den

CHAPTER 5

FINGERPRINTS OF CNS DRUG EFFECTS: A PLASMA NEUROENDOCRINE REFLECTION OF D_2 RECEPTOR ACTIVATION USING MULTI-BIOMARKER PK/PD MODELING

Willem J van den Brink, Dirk-Jan van den Berg, Floor EM Bonsel, Robin Hartman, Yin-Cheong Wong, Piet H van der Graaf, Elizabeth CM de Lange

Published in British Journal of Pharmacology 2018 175:3832-3843

Abstract

Because biological systems behave as networks multi-biomarker approaches increasingly replace single-biomarker approaches in drug development. To improve the mechanistic insights into CNS drug effects, a plasma neuroendocrine fingerprint was identified using multi-biomarker pharmacokinetic/pharmacodynamic (PK/PD) modeling. Short- and longer-term D_2 receptor activation was evaluated using quinpirole as paradigm compound.

Rats (n=44) received 0, 0.17 or 0.86 mg/kg of the D_2 agonist quinpirole intravenously. Quinpirole concentrations in plasma and brain extracellular fluid ($brain_{ECF}$), as well as plasma concentrations of 13 hormones and neuropeptides, were measured. Experiments were performed at day 1 and repeated after seven-day subcutaneous drug administration. PK/PD modeling was applied to identify the *in vivo* concentration-effect relations and neuroendocrine dynamics.

The quinpirole pharmacokinetics were adequately described by a two-compartment model with an unbound $brain_{ECF}$-to-plasma concentration ratio of 5. The release of adenocorticotrophic hormone (ACTH), growth hormone (GH), prolactin (PRL), and thyroid stimulating hormone (TSH) from the pituitary was influenced. Except for ACTH, D_2 receptor expression levels on the pituitary hormone-releasing cells predicted the concentration-effect relationship differences. Baseline levels (ACTH, PRL, TSH), hormone release (ACTH), and potency (TSH) changed with treatment duration.

The integrated multi-biomarker PK/PD approach revealed a fingerprint reflecting D_2 receptor activation. This forms the conceptual basis for *in vivo* evaluation of on- and off-target CNS drug effects. The effect of treatment duration is highly relevant given the long-term use of D_2 agonists in clinical practice. Further development towards quantitative systems pharmacology models will eventually facilitate mechanistic drug development.

Keywords: CNS drugs, neuroendocrine system, biomarkers, quantitative systems pharmacology, dopamine agonists, PK/PD modeling

Abbreviations

ACTH: adenocorticotropic hormone; BBB: blood-brain-barrier; BDNF: brain-derived neurotropic factor; CNS: central nervous system; CRH: corticotropic releasing hormone; FSH: follicle stimulating hormone; GH: growth hormone; LH: luteinizing hormone; OFV: objective function value; PK/PD: pharmacokinetic/pharmacodynamic; PRL: prolactin; RSE: relative standard error; TIDA: tuberoinfundibular dopaminergic; TSH: thyroid stimulating hormone

1. Introduction

Besides insufficient information on drug distribution into and within the brain, a main cause of attrition in central nervous system (CNS) drug development is the lack of translational pharmacodynamic biomarkers, i.e. preclinical biomarkers that are predictive for clinical effect [1–3]. This enables the mechanistic extrapolation of drug effects from animals to humans [3,4].

It is important that these biomarkers are accessible in humans. This poses a challenge for CNS drug development, given that sampling from the human brain is highly limited. However, the pituitary hormones and peptides of the neuroendocrine system are released upon signals from the CNS, in particular the hypothalamus, providing an opportunity to study central drug effects in plasma. Dopamine, for example, is released from the tuberoinfundibular dopamine (TIDA) neurons into the median eminence of the pituitary to control the release of prolactin (PRL) from the lactotrophs into plasma [5]. It has been shown that dopamine D_2 agonists stimulate the release of dopamine into the median eminence [6,7]. This principle has been used to evaluate the dopaminergic drug efficacy with PRL [8–13], including the translation of these effects from rats to humans [10,12].

Realizing that biological systems behave as networks, single biomarker approaches are increasingly replaced by multi-biomarker approaches [14,15]. Although PRL is a sensitive biomarker for dopamine D_2 receptor activation, it is also sensitive to serotonin and thyroid releasing hormone [16]. A multi-biomarker approach is envisioned to provide a more specific reflection of D_2 receptor activation. Indeed, the dopaminergic system has multiple connections to the neuroendocrine system, including the release of PRL, growth hormone (GH), and thyroid stimulating hormone (TSH) [17,18]. With that, it is important to identify the pharmacokinetic/pharmacodynamic (PK/PD) parameters that can be scaled from animals to humans [4]. Moreover, dopaminergic drug effects may change with increasing duration of treatment following sensitization and tolerance, as was shown for D_2 agonists [19].

The aim of the current study was, therefore, to characterize both the short-term and longer-term interaction of the dopaminergic system with the neuroendocrine system, in order to obtain a fingerprint biomarker of D_2 receptor activation. The selective $D_{2/3}$ agonist quinpirole will be used as a paradigm compound. Here we present a PK/PD fingerprint of quinpirole with adenocorticotrophic hormone (ACTH), GH, PRL and TSH as neuroendocrine biomarkers.

2. Methods

2.1. Animals, surgery, and experiment

Animals. Animal studies were performed in agreement with the Dutch Law of Animal Experimentation and approved by the Animal Ethics Committee in Leiden, the Netherlands (study protocol DEC12247). Male Wistar rats (n = 44) were housed in groups for 6-9 days until surgery (Animal Facilities Gorlaeus Laboratories, Leiden, The Netherlands). Animals were held under standard environmental conditions while artificial daylight was provided from 7:30 AM to 7:30 PM. They had ad libitum access to food (Laboratory chow, Special Diets Services, Tecnilab BMI, Someren, The Netherlands) and acidified water.

Surgery. The surgery was performed following previously reported procedures [20]. The rats received 2% isoflurane anesthesia while undergoing surgery. After induction of the isoflurane, 0.09 ml Buprecare® (AST Farma B.V., Oudewater, The Netherlands) was administered intramuscular. Cannulas were placed in the femoral artery for serial blood sampling and the femoral vein for drug administration. Probe guides (CMA/12) with dummy probes were implanted in caudate putamen in both hemispheres (1.0 mm anterior, 3.0 mm lateral, 3.4 mm ventral, relative to bregma) and replaced by the probes (CMA/12 Elite – 4 mm) 24 hours before the experiment. After the surgery, the animals received 0.15 ml Ampicillan® (Dechra Veterinary Products B.V., Bladel, The Netherlands) and 3 ml 0.9% NaCl subcutaneously. The rats were individually held in Makrolon type 3 cages for 7 days to recover and weighed on a daily basis to evaluate the recovery.

Experiments. The rats were randomly assigned to receive 0 (n=12), 0.17 mg/kg (n=16), or 0.86 mg/kg (n=16) intravenous quinpirole between 10:45 AM and 11:15 AM on the first experiment day. The smaller group size for the control group was chosen, because less variation was expected in the data; i.e. there is no inter-individual variation from PK and the resultant PD processes. The statistical non-linear mixed effect analysis (see section *2.3. Data analysis*) is able to handle unbalanced study designs. The microdialysate samples were collected from -200 to 180 minutes (20-minute interval, 1.5 ul/min, 120 min equilibration time) in polypropylene microvolume inserts (250 ul, Waters) containing an antioxidant mix of 10 ul 0.02M formic acid/0.04% ascorbic acid in water. Blood samples of 200 ul were collected in heparin-coated Eppendorf tubes at -5, 5, 7.5, 10, 15, 25, 45, 90, 120 and 180 min and centrifuged (1000 x g, 10 min, 4°C) to separate the plasma. All samples were stored at -80°C until analysis. After the experiment, the cannulas were filled with a saline-heparin solution (venous) or a PVP-heparin solution (arterial), while a dummy replaced the probes. The rats received their quinpirole dose subcutaneously, until the second experiment on day 8, which was executed as on day 1. After the experiment, the rats were sacrificed following an overdose of Nembutal®.

2.2. Chemical analysis of the samples

2.2.1. Quinpirole analysis in plasma and microdialysate

Quinpirole (Bio-Connect, Huissen, The Netherlands) was analyzed using liquid chromatography-tandem mass spectrometry (LCMS/MS). Calibration standards were prepared in plasma with 0, 5, 10, 20, 50, 100, 200, 400 and 500 ng/ml and in buffered perfusion fluid (bPF) with 0, 0.5, 1, 2, 5, 10, 20, 50, 100, 200 ng/ml quinpirole. Quality controls (QC's) were prepared in plasma with 5, 10, 50 and 500 ng/ml and in bPF with 1, 6, 30 and 150 ng/ml quinpirole. Of the microdialysate samples, 20 µL was transferred to microvolume inserts (BGB Analytik, Harderwijk, the Netherlands and spiked with 20 µL of 40 ng/ml internal standard ropinirole-D4 (Bio-Connect, Huissen, the Netherlands). Of the plasma samples, 20 µL was spiked with 20 µL of the same internal standard and 20 µL water before deproteination with 1 mL acetonitrile (AcN). After centrifuging (20,000 x g, 10 min), the supernatant was transferred to an Eppendorf vial and dried by CentriVap vacuum centrifugation (Labconco, Kansas City, Missouri). The residue was dissolved in 40 µL 5 % AcN. After centrifuging (20,000 x g, 10 min) the supernatant was transferred to microvolume inserts and inserted into 1.5 ml screw cap vials.

The vials were placed into the Nexera X2 UHPLC-MS/MS system (Shimadzu, 's Hertogenbosch, the Netherlands) at 10°C. 5 µl of the sample was injected into the system, operated by LCQuan software (version 2.7, Thermo Fisher Scientific, Breda, the Netherlands)) and the MS Finnigan TSQ quantum ultra-mass spectrometer (Thermo Fisher Scientific, Breda, The Netherlands), operated by XCalibur software (version 2.5, Thermo Fisher Scientific, Breda, The Netherlands). An Acquity UPLC BEH C18 column (130Å, 1.7 µm, 2.1 mm X 50 mm; Waters, Etten-Leur, The Netherlands) was used with a flow rate of 0.4 ml/min and a column temperature of 40°C. The mobile phases were prepared in 10 mM ammonium acetate in water (adjusted to pH 7 with formic acid). The aqueous mobile phase (MP_{AQ}) contained 5% and the organic mobile phase (MP_{ORG}) 95% AcN. A gradient was applied with 10% MP_{ORG} (0 – 0.5 min) to 100% MP_{ORG} (0.5 – 2.0 min) and kept at 100% MP_{ORG} (2.0 – 2.8 min), after which the column was re-equilibrated with 10% MP_{ORG} (2.8 – 3.0 min). The retention time of quinpirole and ropinirole-D4 was 1.8 and 2.24 minutes, respectively. The MS was used in positive electrospray ionization mode and all compounds were monitored by Selective Reaction Monitoring (SRM). The ionization voltage, capillary energy, capillary temperature and desolvation temperature were set to 3.50 kV, 3 V, 150°C, and 400°C, respectively. The transition ion pair was 220.18 m/z → 161.00 m/z, 16 V for quinpirole and 265.22 m/z → 132.07 m/z, 32 V for ropinirole-D4. The quality of the method was assured following the guidelines for bioanalysis [21]. The unbound fraction of quinpirole in plasma was determined to be 71 ± 3% (concentration-independent) by filtrating plasma samples using high-speed filtration (Centrifree®, Merck Millipore, Amsterdam, The Netherlands, 2000 x g, 10 min) and calculating the ratio of unbound to total plasma concentrations.

The measured total plasma concentrations of quinpirole were corrected accordingly, to obtain unbound plasma concentrations. The recovery of quinpirole over the microdialysis probe was determined to be 5.4 ± 1.7% (n = 191) using the retrodialysis method [22]. The measured microdialysate quinpirole concentrations were corrected for probe recovery to report the $brain_{ECF}$ concentrations.

2.2.2. Pituitary hormones and neuropeptides in plasma

The pituitary hormones (ACTH, brain-derived neurotropic factor (BDNF), follicle stimulating hormone (FSH), GH, luteinizing hormone (LH), PRL and TSH) and neuropeptides (α-melanocyte stimulating hormone, β-endorphin, neurotensin, Orexin A, oxytocin, Substance P) were analysed by multiplex assays (RTPMAG-86K and RMNPMAG-83k, Merck Millipore, Darmstadt, Germany) on a Bio-Plex® MAGPIX™ system (BioRad Laboratories, Veenendaal, The Netherlands). With the RTPMAG-86k, 10 uL and with the RMNPMAG-83k, 50 uL plasma was used for analysis according to the protocol provided by the manufacturer.

2.3. Data analysis

2.3.1. PK/PD modeling software and criteria

The PK/PD models to describe the quinpirole and the hormone concentrations in $brain_{ECF}$ and plasma were developed by a two-stage approach (the PK parameters were fixed before developing the PD models), using a non-linear mixed effect population approach in NONMEM® version 7.3.0 with subroutine ADVAN13. The inter-individual variability around the parameters and the residual error were described by an exponential distribution (suppl. Equation 1, 2). Model selection was based on successful convergence, objective function value (OFV), parameter precision and visual evaluation of the model predictions as compared to the observations.

2.3.2. Pharmacokinetic model development

Two- and three-compartment models were compared, both with linear or non-linear clearance from plasma for their description of unbound quinpirole concentrations in plasma and $brain_{ECF}$. Here it should be noted that a two-compartment model refers to one compartment describing plasma and another compartment describing $brain_{ECF}$ quinpirole concentrations. The transport into and out of the brain across the blood-brain-barrier (BBB) in these models was estimated with two separate distribution clearances. The experiment day was evaluated as covariate on one of the model parameters. The selected model was evaluated on additional data to guarantee external validity, and the details of which are described in the supplementary information.

2.3.3. Pharmacodynamic model development

For each hormone, baseline, PK/PD and covariate models were developed in a step-wise manner. Baseline patterns were evaluated on placebo data following supplementary equations Part I, 4 – 7. The selected baseline models were, together with the pharmacokinetic model, integrated into the PK/PD models. The PK/PD models were defined as a combination of the following characteristics: i) baseline model for each hormone; ii) plasma or $brain_{ECF}$ as target site; iii) the slope, the E_{MAX}, the alternative E_{MAX} [23], the on-off, or no drug effect model; iv) and the direct response, the turnover or the pool model as link model (suppl. Equations Part I, 9-16). The best model was automatically selected on basis of model convergence and OFV. Finally, the selected PK/PD models were evaluated for an effect of experiment day using step-wise covariate model building [24] (suppl. Equations Part I, 17-19).

2.3.4 Estimation of signal transduction efficiency

The quantitative relation between receptor binding and pharmacological effect depends on the signal transduction efficiency [25,26], which is made explicit in the operational model of agonism [27]. Therefore, the selected PK/PD models were simulated and fitted by the operational model (Equation 1) [25,27]:

$$E = \frac{E_m * \tau * C}{k_A + (1 + \tau) * C} \quad (1)$$

In which E_m is the systems maximum, τ is the transduction efficiency, and k_A is the affinity for the D_2 receptor. It was assumed that the target site of action is in the $brain_{ECF}$. Furthermore, the assumption was made that quinpirole is selective for the dopamine D_2 receptor, and the GH, PRL and TSH responses were modulated via the TIDA neurons (Figure 2). Therefore, the affinity of quinpirole to the D_2 receptor was estimated equal among all hormones, while the signal transduction efficiency of GH, PRL and TSH was assumed dependent on pituitary D_2 receptor expression obtained from literature [28]. The D_2 receptor expression for somatotrophs, lactotrophs and thyrotrophs was calculated as the number of 'troph' cells expression the D_2 receptor relative to the total number of 'troph' cells. This relation to the signal transduction efficiency was made explicit following equation 2:

$$\tau = \tau_0 * e^{slp * receptor\ expression} \quad (2)$$

Where τ is estimated for GH, PRL and TSH on basis of the pituitary D_2 receptor expression.

3. Results

3.1. Pharmacokinetics of quinpirole in plasma and brain$_{ECF}$

A two-compartment model best described the pharmacokinetics of quinpirole in plasma and brain$_{ECF}$ with linear first-order elimination from plasma and a net active influx from plasma to brain$_{ECF}$ (Suppl. Equation 3). The parameter estimates were precise and accurate (Table I), and the model could well describe the quinpirole concentrations in plasma and brain$_{ECF}$ over a large dose range (Figure 1A). Although there is a slight over-prediction of quinpirole concentrations in brain$_{ECF}$, external validation showed good extrapolative ability of the model (Figure 1B).

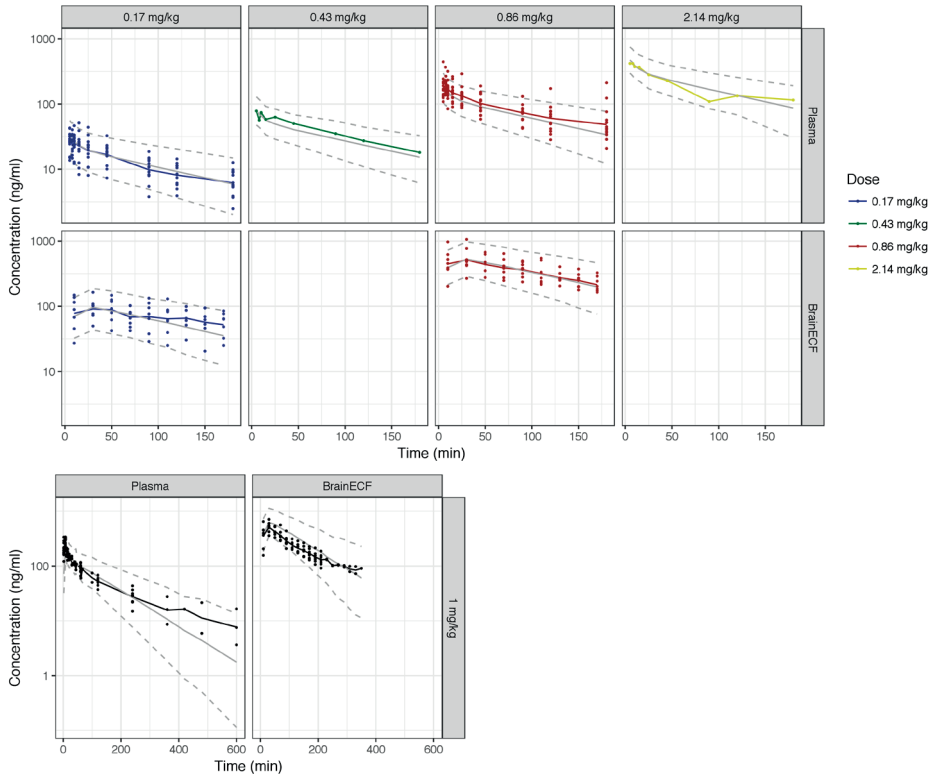

Figure 1. Visual predictive check (A) and external validation (B) for the quinpirole pharmacokinetic model in plasma and brain$_{ECF}$. The colored dots represent the observed data, with the solid colored lines showing the mean of the observations. The solid grey line shows the mean, and the dashed grey lines the 90% confidence interval of 500 simulations. *The experiments in which the animals received 0.43 mg/kg and 2.14 mg/kg represented experimental protocol deviations (higher dose), and were included in PK model development only.

Table I. Parameter estimates of the quinpirole pharmacokinetic model

Parameter	Model evaluation		Bootstrap (n_{btstr} = 168)	
	Estimate	(RSE)[shr]	Estimate	(CV)
$CL_{PL,o}$ (L h^{-1})	0.71	(9%)	0.70	(9%)
IIV $CL_{PL,o}$	0.12	(32%) [7%]	0.12	(35%)
$CL_{PL,ECF}$ (L h^{-1})	2.5	(20%)	2.5	(19%)
$CL_{ECF,PLASMA}$ (L h^{-1})	0.52	(24%)	0.55	(24%)
$k_{p,uu}$ ($CL_{PL,ECF}$/$CL_{ECF,PL}$)	5			
$V_{CENTRAL}$ (L)	1.0	(6%)	1.0	(7%)
V_{ECF} (L)	0.12	(13%)	0.013	(17%)
RUV $C_{QP,PL}$	0.08	(24%) [3%]	0.08	(24%)
RUV $C_{QP,ECF}$	0.12	(28%) [2%]	0.12	(30%)

C: concentration; CL: clearance; CV: coefficient of variation; ECF: brain extracellular fluid; h: hour; IIV: inter-individual variability; $k_{p,uu}$: ratio of unbound $brain_{ECF}$ and plasma drug concentration; L: liter; n_{btstr}: number of successful bootstrap model runs out of a total of 200 runs; PL: plasma; RSE: relative standard error; RUV: residual unexplained variability; shr: shrinkage; V: volume of distribution

3.2.1. Responding pituitary hormones and neuropeptides in plasma

On basis of automated model selection, the hormones luteinizing hormone, PRL and TSH showed a placebo response described by circadian rhythm with a period of 120 minutes, the Bateman equation, or exponential decay, respectively (Suppl. Figure 1A). A model with no baseline pattern best described the other hormone baselines. ACTH, GH, PRL and TSH responded to quinpirole treatment with diverse PK/PD relations, while no effect was observed on the neuropeptides, BDNF, FSH and LH, following automated model selection (Suppl. Figure 1B, Table II). Except for $k_{deg,ACTH}$ (relative standard error (RSE) = 282%) and $EC_{50,Prl}$ (RSE = 99%), the parameters were identified with reasonable precision (Table III) and the models could describe the data well (suppl Equations Part II, suppl. Figure 2).

Table II. The PK/PD effects of quinpirole on ACTH, GH, PRL and TSH, including the PK/PD model type and target site of drug action that was identified

Hormone	Effect	PK/PD model	Target site
ACTH	+	Slope model & Pool model with stimulation of k_{REL}	Plasma
GH	-	E_{MAX} model & Turnover model with inhibition of k_{REL}	$Brain_{ECF}$
PRL	-	E_{MAX} model & Turnover model with inhibition of k_{REL}	$Brain_{ECF}$
TSH	-	E_{MAX} model & Turnover model with inhibition of k_{REL}	$Brain_{ECF}$

ACTH: adenocorticotropic hormone; ECF: extracellular fluid; Effect: + increased release, - reduced release; GH: growth hormone; k_{REL}: hormone release rate; PRL: prolactin; TSH: thyroid stimulating hormone

3.2.2. Target site of effect

No statistically significant difference was identified comparing the best models for ACTH, GH, PRL and TSH with either plasma or $brain_{ECF}$ as target site (Table III).

Table III. Parameter estimates of the PK/PD models for quinpirole effect on ACTH, GH, PRL and TSH with plasma and $brain_{ECF}$ as target site. In bold the parameters of the selected models.

	Plasma	**$Brain_{ECF}$**
ACTH	**Estimate (RSE)**	**Estimate (RSE)**
OFV	-31.3	-32.9
Baseline (pg/ml)	3.74 (17%)	3.71 (17%)
$IIV_{Baseline}$	0.68 (71%) [0%]	0.68 (72%) [0%]
Slope ($[ng/ml]^{-1}$)	0.873 (43%)	-
E_{MAX}	-	2.35 (11%)
EC_{50} (ng/ml)	-	54.1 (40%)
K_{DEG} (min^{-1})	0.0146 (24%)	308 (282%)
K_{REL} (min^{-1})	0.00760 (29%)	0.00421 (31%)
RUV	0.27 (21%) [3%]	0.27 (21%) [3%]
GH		
OFV	667.6	664.1
Baseline (pg/ml)	1002 (n.a.)	992 (25%)
E_{MAX}	-1 (n.a.)	-1 (39%)
S_0 ($[ng/ml]^{-1}$)	0.0545 (n.a.)	0.00985 (53%)
EC_{50} (ng/ml)	18.4 (calc.)	101 (calc.)
K_{DEG} (min^{-1})	0.0228 (n.a.)	0.0282 (22%)
RUV	2.48 (13%)	2.45 (13%)
PRL		
OFV	377.0	373.5
Baseline (pg/ml)	284 (25%)	262 (25%)
$IIV_{Baseline}$	0.70 (28%) [4%]	0.67 (28%) [4%]
D_{Plac} (pg/ml)	8.72 (fix)	8.72 (fix)
$K_{IN,\ Plac}$ (min^{-1})	1.65 (fix)	1.65 (fix)
$K_{DEC,\ Plac}$ (min^{-1})	1.55 (fix)	1.55 (fix)
E_{MAX}	-0.961 (21%)	-0.959 (13%)
EC_{50} (ng/ml)	0.0983 (275%)	0.933 (99%)
K_{DEG} (min^{-1})	0.584 (22%)	0.0652 (22%)
RUV	0.79 (18%) [3%]	0.79 (18%) [3%]
TSH		
OFV	-272.2	-270.0
Baseline (pg/ml)	305 (5.3%)	293 (4.7%)
$IIV_{Baseline}$	0.047 (30%) [8%]	0.045 (30%) [9%]

Table III. Parameter estimates of the PK/PD models for quinpirole effect on ACTH, GH, PRL and TSH with plasma and brain$_{ECF}$ as target site. In bold the parameters of the selected models. (continued)

	Plasma	Brain$_{ECF}$
ACTH	**Estimate (RSE)**	**Estimate (RSE)**
$K_{DEC, Plac}$ (min^{-1})	0.00489 (fix)	0.00489 (fix)
E_{MAX}	-0.819 (36%)	-0.794 (32%)
EC_{50} (ng/ml)	31.2 (30%)	178 (34%)
K_{DEG} (min^{-1})	0.0781 (13%)	0.126 (20%)
RUV	0.17 (19%) [2%]	0.18 (19%) [2%]

ACTH: adenocorticotropic hormone; D_{Plac}: the extent of the placebo effect; ECF: extracellular fluid; EC_{50}: concentration at half maximal drug effect; E_{MAX}: maximal drug effect; GH: growth hormone; k_{DEC}: dose-independent hormone decay; k_{DEG}: hormone elimination rate; k_{REL}: hormone release reate; OFV: objective function value; PRL: prolactin; RSE: relative standard error; RUV: residual unexplained variability; S_0: E_{MAX}/ EC_{50}; TSH: thyroid stimulating hormone

3.2.3. Mechanistic evaluation of quinpirole effect on ACTH, GH, PRL, and TSH

The concentration-effect relations between quinpirole and every single hormone are depicted in Figure 3, assuming brain$_{ECF}$ as target site (table III). Prolactin was most sensitive to quinpirole with a potency of 0.93 ng/ml, while ACTH, GH and TSH responded with a potency of 54 ng/ml, 101 ng/ml and 178 ng/ml, respectively (Table III). The operational model could fit the simulated concentration-effect relationships well (Figure 3, Table IV). Within this model, the signal transduction efficiency values (τ) of GH, PRL and TSH could be related to the pituitary receptor expression on the somatotrophs, lactotrophs and the thyrotrophs, respectively. In contrast, the ACTH concentration-response relationship could not be fitted under the assumption of signal transduction efficiency being dependent on pituitary D_2 receptor expression (suppl. Figure 3).

3.2.4. One-day versus eight-day treatment responses

The pharmacokinetics of quinpirole were not significantly influenced by eight-day drug treatment. In contrast, the pharmacodynamics showed a significant change for ACTH, PRL and TSH (suppl. Table I). The differences between the responses after short- and long-term treatment are graphically presented in Figure 4. The basal levels of ACTH were increased independent of dose, while the hormone release rate was increased in a dose-dependent manner. This resulted in a lower maximal ACTH response after 8-day treatment with a high dose as compared to a low dose of quinpirole. The basal PRL concentrations after eight days were increased with dose, while the extent of the placebo effect was decreased, independent of dose. The basal levels of TSH have decreased with eight-day treatment regardless the dose, while the sensitivity to quinpirole (EC_{50}) was decreased in a dose-dependent manner.

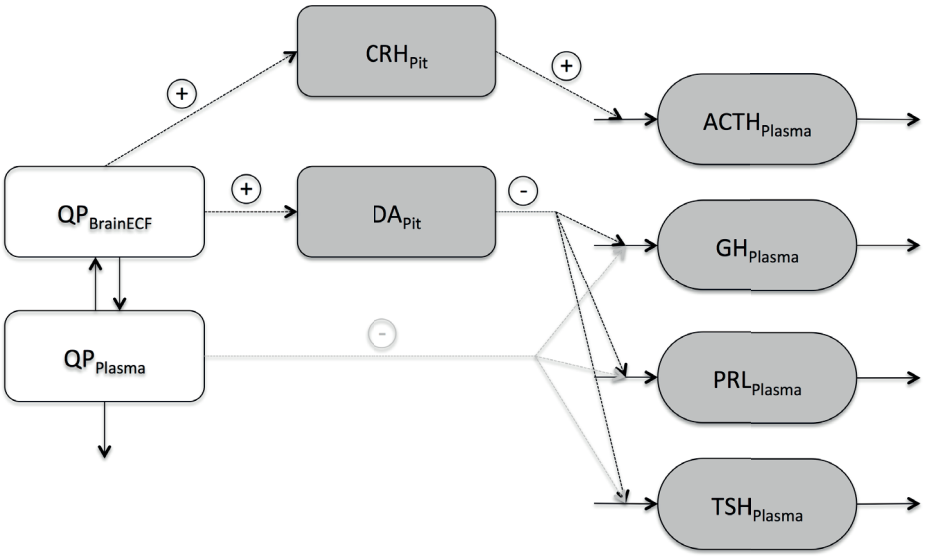

Figure 2. The interaction between quinpirole and the neuroendocrine system with the pharmacokinetics as white compartments and the pharmacodynamics as grey compartments. Quinpirole stimulates TIDA neurons in the hypothalamus to increase the release of dopamine into the pituitary. Dopamine inhibits the release of GH, PRL and TSH into plasma. ACTH was stimulated by quinpirole, suggesting a pathway other than TIDA neuron stimulation. The main effect site is assumed to be the brain, given the high quinpirole in brain$_{ECF}$ as compared to plasma. QP: quinpirole; DA: dopamine; CRH: corticotropic releasing hormone; ACTH: adenocorticotropic hormone; GH: growth hormone; PRL: prolactin; TSH: thyroid stimulating hormone.

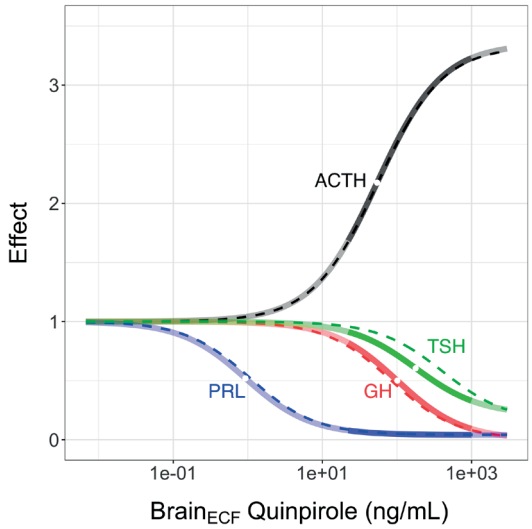

Figure 3. A) Simulated concentration-effect relations for ACTH (black), TSH (green), GH (red) and PRL (blue) on basis of the parameter estimates in table III. The dark segments represent the quinpirole concentration range measured in brain$_{ECF}$. The dotted lines represent the fit with the operational model, in which the signal transduction efficiency τ for GH, PRL and TSH is dependent on D_2 receptor expression following equation 2.

Table IV. Relative D_2 receptor expression on the troph cells in the rat anterior pituitary, the signal transduction efficiency τ, and the systems maximal effect E_m estimated from the operational model in equation 1. The k_A was estimated 805 ng/ml (see equation 1), while the τ_{GH}, τ_{PRL}, τ_{TSH} was described by $\tau=0.24*e^{0.106*receptor\ expression}$

	D_2 receptor expression [28]	τ	E_M
Corticotrophs (ACTH)	20%	13.8	2.51
Somatotrophs (GH)	34%	8.7	-1.11
Lactotrophs (PRL)	76%	743	-0.96
Thyrotrophs (TSH)	13%	0.94	-1.76

ACTH: adenocorticotropic hormone; GH: growth hormone; PRL: prolactin; TSH: thyroid stimulating hormone

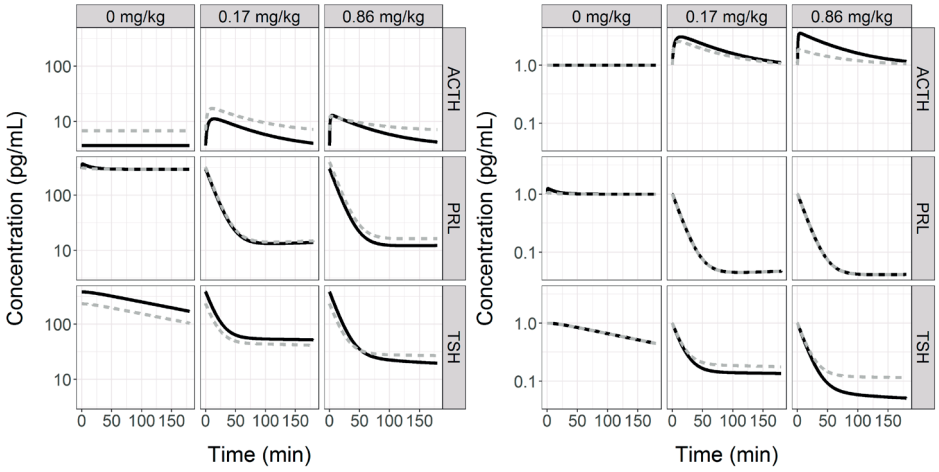

Figure 4. Simulated hormone actual (A) and baseline normalized (B) concentration-time profiles of ACTH, PRL and TSH after one administration (solid black line) and 8 administrations (dashed grey line).

4. Discussion and conclusion

This study systematically evaluated the effects of quinpirole on the neuroendocrine system following a PK/PD based multi-biomarker approach. Quinpirole showed a high rate of transport over the blood-brain-barrier with an unbound partition coefficient ($k_{p,uu}$) of 5. ACTH, GH, PRL, and TSH responded to quinpirole, each with a unique target site concentration-effect relationship, providing a fingerprint of D_2 receptor activation. Additionally, while no changes were found in PK, the pharmacodynamics changed with eight-day administration both dependent and independent of the quinpirole dose. This study underlines the need for integrative multi-biomarker evaluations of drug effects to comprehend the system-wide pharmacological profile.

4.1. Can the target site of effect be determined?

Since the ultimate purpose is to identify peripheral biomarkers of the central drug effect, an important question is whether we can consider $brain_{ECF}$ concentrations as the target site concentrations of the effect of quinpirole. We have shown that, on basis of statistical significance, it was not possible to discriminate between $brain_{ECF}$ or plasma as target site of effect. Given that the D_2 receptors on the 'troph' cells are accessible from plasma, and the release of these hormones have been modified by systemic dopamine infusion [29,30], it is suggested that these hormones are released upon peripheral drug action. On the other hand, the release of these hormones is tightly controlled by signals from the hypothalamus that are highly connected to dopamine and other neurotransmitter systems. Considering this, the rate and extent of drug distribution into the brain may determine the dominant target site of effect. For the D_2 antagonist remoxipride ($k_{p,uu}$ = 1) [11]) , $brain_{ECF}$ could be considered as target site to release PRL into plasma, while for the D_2 antagonist risperidone ($k_{p,uu}$ = 0.45 [31]), plasma could be considered as target site [10,11,32]. Quinpirole is found to be subjected to active influx: although no information on the transporter is available in literature, it is observed that, under steady state conditions, the free drug concentration in $brain_{ECF}$ is as much as five times higher than in plasma ($k_{p,uu}$ = 5, Table I). Therefore, although we could not provide a statistical determination, it is presumed that the main effect of quinpirole on the neuroendocrine system is mediated via the brain rather than via the periphery.

4.2. Interpretation of the unique concentration-effect relationships

Dopamine activity in the brain is reflected in the tuberoinfundibular dopamine pathway that consists of three types of neurons that project from the hypothalamus to the pituitary: 1) the TIDA neurons; 2) the periventricular hypophyseal dopamine neurons, and 3) the tuberohypophyseal dopamine neurons [5]. TIDA neurons release dopamine into the long portal veins of the pituitary to which the 'troph' cells are exposed. While quinpirole has affinity for both the D_2 and the D_3 receptor [33], the effects on the neuroendocrine system are putatively mediated via the D_2 receptor because of the following findings. First, , the enhancing effect of quinpirole on ACTH release was reversed with administration of the D_2 receptor antagonist sulpiride [34,35]. Second, the effect of quinelorane, which is similarly specific for the $D_{2/3}$ receptor, on the neuroendocrine TIDA neurons was antagonized by the selective D_2 receptor antagonist raclopride [6]. Third, while the selective D_2 agonist PNU-95,666 activated the TIDA neurons and inhibited PRL release, this was not the case for the selective D_3 agonist PD128907 [7]. In contrast, studies with selective D_2 and D_3 agonists in ovariectomized estrogen-primed female rats showed a decrease of TIDA neuron activity and an increase of subsequent PRL release [36,37]. However, the estrogen-priming in these studies prevents a direct comparison between these results and our results, since estrogen interferes with TIDA neuron activity as well as the sensitivity of

the pituitary to dopamine [38,39]. Indeed, our study design is more similar to that of the studies observing activation of TIDA neuron activity and suppression of PRL release, i.e. they studied male rats, or diestrous female rats with low estrogen levels [6,7]. Therefore, we assume that the stimulation of TIDA neuron activity by of quinpirole in our study is D_2 specific. Dopamine D_2 receptors were identified not only on lactotrophs (PRL), but also on corticotrophs (ACTH), somatotrophs (GH), gonadotrophs (FSH, LH), and thyrotrophs (TSH) [17,28]. Also, dopamine agonists inhibited the release of ACTH, GH, PRL and TSH *in vitro*, likely mediated via the D_2 receptors [40–42]. Overall, it is thus expected that ACTH, GH, PRL, and TSH concentrations decrease with quinpirole treatment upon the stimulation of TIDA neuron activity that enhances dopamine release into the pituitary to bind to the pituitary dopamine receptors on the 'troph' cells. Interestingly, the secretion of ACTH was increased, indicating a different mechanism of action not via the TIDA neurons. The hypothalamic mediator of ACTH release is corticotrophin-releasing hormone (CRH). CRH is under control of several neurotransmitters, for example, norepinephrine and gamma-aminobutyric acid. Since the effect of quinpirole on ACTH was found to be D_2 receptor specific [34], it is likely that CRH or the controlling neurotransmitters are influenced in a D_2 specific manner (Figure 2).

According to these mechanisms the assumptions of D_2 receptor selectivity for all hormones and the pituitary D_2 receptor expression dependent signal transduction for GH, PRL and TSH were made (Figure 2, Table IV). Conceptually, the differences in signal transduction efficiency may also be explained by differences in fractional receptor occupancy needed to elicit a certain level of pituitary hormone release, i.e. the release of some hormones may be more sensitive dopamine receptor activation than that of other hormones. However, our assumptions are confirmed by a good fit of the operational model on the simulated concentration effect relationships as depicted in Figure 3. Physiologically, this suggests a receptor expression dependent sensitivity of the hormones to the increase of pituitary dopamine following the central quinpirole effect. In fact, it indicates that τ indeed is a system-specific parameter. The opposed direction of the ACTH response, and the deviation of τ_{ACTH} from the relation between receptor expression and τ indicates a different mechanism of action of D_2 receptor activation on ACTH release (Figure 3, Table IV, suppl. Figure 3). Altogether, the systems response expressed in terms of signal transduction efficiency provides a fingerprint that is specific for D_2 receptor stimulation in the brain.

4.3. Habituation, tolerance and homeostatic feedback mechanisms

There are three mechanisms through which the differences between day 1 and day 8 are explained (Figure 4). First of all, the dose-independent changes are likely the consequence of habituation; the animals' response to the daily injection procedure returns to basal levels with longer-term administration. Indeed, the ACTH and TSH basal levels and the

PRL placebo response changed over the period of quinpirole administration (Figure 4). Second of all, pharmacodynamic tolerance may occur as a consequence of long-term drug administration [43]. Tolerance is the mechanism of physiological adaptation to continuous external stimuli, for example, the change in receptor expression. Pharmacodynamic tolerance was identified for the TSH response, as indicated by the dose-dependent change of EC_{50} (Figure 4, suppl. Table I). Assuming a D_2 dependent mechanism, this cannot be explained by reduced hypothalamic D_2 receptor expression, since this was not observed for the other hormones. Moreover, D_2 receptor expression was found not to change with long-term D_2 agonist exposure [44]. Possibly, the balance between other mediators of TSH release and dopamine has changed, thereby influencing the transduction efficiency. Third of all, the differences between the experiment days can be explained by homeostatic feedback mechanisms. The release rates of ACTH and PRL were increased in a dose-dependent manner, suggesting a positive and negative feedback, respectively (Figure 4, Suppl. Table I). These hormones are components of highly complex networks that include multiple negative and positive feedback mechanisms that are affected by eight-day administration of quinpirole. The net effect is reflected in the current analysis, showing that these networks have changed to another equilibrium.

4.5. Strengths, limitations and future research

Our integrated PK/PD approach included multiple hormones and neuropeptides that provide comprehensive insight into the interaction between quinpirole and the neuroendocrine system to reveal a fingerprint reflecting D_2 receptor activation. Nevertheless, it has a few limitations that will be discussed in this section. First of all, the 3-hour duration of the experiments limited the evaluation of the full pharmacodynamic response. While ACTH levels were back to baseline at the end of the experiment, GH, PRL and TSH levels were still decreased. This may have limited the precise identification of the PK/PD model, although, in general, the parameter estimates showed good precision. Second, a wider dose range may have enabled better identification of the EC_{50} parameter in case of, for example, ACTH that was best described by a slope model. However, since a relatively untargeted approach was applied, it was not possible to anticipate the dose range beforehand. Moreover, the current choice of doses was based on an experimental regimen, reflecting the therapeutic range [45,46], in order to gain pharmacologically relevant insights. Third, the choice of hormones and neuropeptides, although guided by pharmacological knowledge, was based on the available platforms rather than based on the physiology. While this provides a non-biased evaluation of neuroendocrine effects of quinpirole, there is a series of hormones that will be of interest for further research, for example, the downstream signals of the pituitary hormones, such as will be discussed below.

Suggestions for further investigation include the validation of the D_2 receptor activation fingerprint with other selective D_2 agonists, for example, quinelorane and ropinirole [33]. Furthermore, we suggest efforts towards unraveling the mechanisms underlying the quinpirole-hormone relationships that were identified in the current study. Such investigation should include: i) the measurement of quinpirole and dopamine in the hypothalamus using microdialysis [47]; ii) the measurement of quinpirole and CRH, GHRH, dopamine, and TRH in the pituitary using microdialysis [48]; iii) the measurement of ACTH, GH, PRL, and TSH in plasma; iv) the measurement of corticosterone, IGF-1, triiodithyronine, thyroxine as downstream signals of ACTH, GH and TSH, respectively; v) a study duration of at least 6 hours of experiment. This takes into account the duration of quinpirole exposure (~4 hours) as well as the delay of the hormone responses.

Such data will form the basis of a quantitative systems pharmacology model describing the interaction between quinpirole and the neuroendocrine system in terms of purely drug- and system-specific parameters. This will also allow the separation of central and peripheral quinpirole effect since the drug concentration will be evaluated in both the hypothalamus and the pituitary. Moreover, the upstream hormones that are released from the hypothalamus will exclusively reflect the hypothalamic interaction with the drug. Eventually, such model can be evaluated with different lengths of chronic administration periods to mechanistically understand the tolerance and homeostatic feedback mechanisms.

4.6. Conclusion

The current study has made the case for an integrated and system-wide approach to understand the interaction between dopaminergic pharmacology and the neuroendocrine system. It was shown that, under standard experimental conditions, quinpirole interferes with the hypothalamus-pituitary-adrenal axis (ACTH), the growth hormone system (GH), parts of the reproductive system (PRL), and the thyroid function (TSH). With this multi-biomarker approach, a fingerprint of transduction efficiency values was obtained that is specific for D_2 receptor activation. In contrast to PRL alone, as classical biomarker, this multi-biomarker fingerprint provides a specific reflection of D_2 receptor activation. Our study also indicated a clear change of the PK/PD relationship with comparing short-term and longer-term administration. This is highly relevant, considering the long-term use of D_2 receptor agonists in clinical practice. Further understanding of the underlying tolerance and homeostatic feedback mechanisms will increase the proper application of these drugs in clinical practice.

In conclusion, this study provided further insights into the interaction between dopaminergic pharmacology and the neuroendocrine system. Using a multi-biomarker approach,

a fingerprint of D_2 receptor activation was obtained. This forms the conceptual basis for the in vivo evaluation of the on- and off-target effects of drug effects in the CNS. Further efforts towards quantitative systems pharmacology model development will eventually lead to mechanistic translational dopaminergic drug development.

Acknowledgements

We would like to thank Fred Koddekee and Anouk Koot for their assistance with the subcutaneous injections and Michiel van Esdonk for his help in automating the model evaluation process.

References

[1] Hurko O, Ryan JL. Translational research in central nervous system drug discovery. NeuroRx. 2005;2:671–682.

[2] Soares HD. The use of mechanistic biomarkers for evaluating investigational CNS compounds in early drug development. Curr. Opin. Investig. Drugs. 2010;11:795–801.

[3] Lange ECM de, Brink WJ van den, Yamamoto Y, et al. Novel CNS drug discovery and development approach: model-based integration to predict neuro-pharmacokinetics and pharmacodynamics. Expert Opin. Drug Discov. 2017;12:1207–1218.

[4] Danhof M, de Lange ECM, Della Pasqua OE, et al. Mechanism-based pharmacokinetic-pharmacodynamic (PK-PD) modeling in translational drug research. Trends Pharmacol. Sci. 2008;29:186–191.

[5] Freeman ME, Kanyicska B, Lerant A, et al. Prolactin : Structure , Function , and Regulation of Secretion. Physiol. Rev. 2000;80:1523–1631.

[6] Eaton MJ, Gopalan C, Kim E, et al. Comparison of the effects of the dopamine D2 agonist quinelorane on tuberoinfundibular dopaminergic neuronal activity in male and female rats. Brain Res. 1993;629:53–58.

[7] Durham RA, Eaton MJ, Moore KE, et al. Effects of selective activation of dopamine D 2 and D 3 receptors on prolactin secretion and the activity of tuberoinfundibular dopamine neurons. Eur. J. Pharmacol. 1997;335:37–42.

[8] Petty RG. Prolactin and antipsychotic medications: Mechanism of action. Schizophr. Res. 1999;35:67–73.

[9] Movin-Osswald G, Hammarlund-Udenaes M. Prolactin release after remoxipride by an integrated pharmacokinetic-pharmacodynamic model with intra- and interindividual aspects. J. Pharmacol. Exp. Ther. 1995;274:921–927.

[10] Stevens J, Ploeger BA, Hammarlund-Udenaes M, et al. Mechanism-based PK-PD model for the prolactin biological system response following an acute dopamine inhibition challenge: Quantitative extrapolation to humans. J. Pharmacokinet. Pharmacodyn. 2012;39:463–477.

[11] Brink WJ van den, Wong YC, Gülave B, et al. Revealing the Neuroendocrine Response After Remoxipride Treatment Using Multi-Biomarker Discovery and Quantifying It by PK/PD Modeling. AAPS J. [Internet]. 2017;19:274–285. Available from: http://link.springer.com/10.1208/s12248-016-0002-3.

[12] Petersson KJ, Vermeulen AM, Friberg LE. Predictions of In Vivo Prolactin Levels from In Vitro K i Values of D2 Receptor Antagonists Using an Agonist–Antagonist Interaction Model. AAPS J. [Internet]. 2013;15:533–541. Available from: http://link.springer.com/article/10.1208/s12248-012-9450-6%5Cnhttp://link.springer.com/content/pdf/10.1208%2Fs12248-012-9450-6.pdf.

[13] Taneja A, Vermeulen A, Huntjens DRH, et al. A comparison of two semi-mechanistic models for prolactin release and prediction of receptor occupancy following administration of dopamine D2 receptor antagonists in rats. Eur. J. Pharmacol. [Internet]. 2016; Available from: http://linkinghub.elsevier.com/retrieve/pii/S0014299916304356.

[14] Greef J Van Der, Mcburney RN. Rescuing drug discovery: in vivo systems pathology and systems pharmacology. Nat. Rev. Drug Discov. 2005;4:961–968.

[15] Greef J van der, Martin S, Juhasz P, et al. The Art and Practice of Systems Biology in Medicine : Mapping Patterns of Relationships. J. Proteome Res. 2007;6:1540–1559.

[16] Lyons DJ, Broberger C. TIDAL WAVES : Network mechanisms in the neuroendocrine control of prolactin release. Front. Neuroendocrinol. [Internet]. 2014;35:420–438. Available from: http://dx.doi.org/10.1016/j.yfrne.2014.02.001.

[17] Pivonello R, Ferone D, Lombardi G, et al. Novel insights in dopamine receptor physiology. Eur. J. Endocrinol. 2007;156:S13–S21.

[18] Tuomisto J, Mannisto P. Neurotransmitter Regulation of Anterior Pituitary Hormones. Pharmacol. Rev. 1985;37:249–332.

[19] Tirelli E, Jodogne C. Behavioral sensitization and tolerance to the D2 agonist RU 24213: Dissociation between several behavior patterns in mice. Pharmacol. Biochem. Behav. 1993;44:627–632.

[20] Westerhout J, Ploeger B, Smeets J, et al. Physiologically Based Pharmacokinetic Modeling to Investigate Regional Brain Distribution Kinetics in Rats. AAPS J. 2012;14:543–553.

[21] Viswanathan CT, Bansal S, Booth B, et al. Quantitative bioanalytical methods validation and implementation: Best practices for chromatographic and ligand binding assays. Pharm. Res. 2007;24:1962–1973.

[22] de Lange ECM. Recovery and Calibration Techniques: Toward Quantitative Microdialysis. Microdialysis Drug Dev. 2013. p. 13–33.
[23] Schoemaker RC, van Gerven JM, Cohen AF. Estimating potency for the Emax-model without attaining maximal effects. J. Pharmacokinet. Biopharm. [Internet]. 1998;26:581–593. Available from: http://eutils.ncbi.nlm.nih.gov/entrez/eutils/elink.fcgi?dbfrom=pubmed&id=10205772&retmode=ref&cmd=prlinks%5Cnpapers3://publication/uuid/37d718a5-1077-492d-a8b0-e29bfbc35f8c.
[24] Khandelwal A, Harling K, Jonsson EN, et al. A Fast Method for Testing Covariates in Population PK/PD Models. AAPS J. [Internet]. 2011;13:464–472. Available from: http://www.springerlink.com/index/10.1208/s12248-011-9289-2.
[25] Danhof M, de Jongh J, De Lange ECM, et al. Mechanism-based pharmacokinetic-pharmacodynamic modeling: biophase distribution, receptor theory, and dynamical systems analysis. Annu. Rev. Pharmacol. Toxicol. 2007;47:357–400.
[26] Jonker DM, Visser SAG, Graaf PH Van Der, et al. Towards a mechanism-based analysis of pharmacodynamic drug – drug interactions in vivo. Pharmacol. Ther. 2005;106:1–18.
[27] Black JW, Leff P. Operational Models of Pharmacological Agonism. Proc. R. Soc. B Biol. Sci. 1983;220:141–162.
[28] Goldsmith PC, Cronin MJ, Weiner RI. Dopamine receptor sites in the anterior pituitary. J. Histochem. Cytochem. 1979;27:1205–1207.
[29] Besses GS, Burrow GN, Spaulding SW, et al. Dopamine infusion acutely inhibits the TSH and prolactin response to TRH. J. Endocrinol. Metab. 1975;41:985–988.
[30] Vance MLEE, Kaiser DL, Frohman LA, et al. Role of Dopamine in the Regulation of Growth Hormone Secretion: Dopamine and Bromocriptine Augment Growth Hormone (GH)-Releasing Hormone-Stimulated GH Secretion in Normal Man. J. Clin. Endocrinol. Metab. 1987;64:1136–1141.
[31] Yamamoto Y, Välitalo PA, Berg D-J van den, et al. A Generic Multi-Compartmental CNS Distribution Model Structure for 9 Drugs Allows Prediction of Human Brain Target Site Concentrations. Pharm. Res. [Internet]. 2016; Available from: http://dx.doi.org/10.1007/s11095-016-2065-3.
[32] Shimizu S, Hoedt SM Den, Mangas-sanjuan V, et al. Target-Site Investigation for the Plasma Prolactin Response : Mechanism-Based Pharmacokinetic-Pharmacodynamic Analysis of Risperidone and Paliperidone in the Rat s. Drug Metab. Dispos. 2017;45:152–159.
[33] Millan MJ, Maiofiss L, Cussac D, et al. Differential actions of antiparkinson agents at multiple classes of monoaminergic receptor. I. A multivariate analysis of the binding profiles of 14 drugs at 21 native and cloned human receptor subtypes. J. Pharmacol. Exp. Ther. 2002;303:791–804.
[34] Borowsky B, Kuhn CM. D1 and D2 dopamine receptors stimulate hypothalamo-pituitary-adrenal activity in rats. Neuropharmacology. 1992;31:671–678.
[35] Kurashima M, Domae M, Inoue T, et al. Inhibitory effects of putative dopamine D3 receptor agonists, 7-OH-DPAT and quinpirole, on prolactin secretion in rats. Pharmacol. Biochem. Behav. [Internet]. 1996;53:379–383. Available from: http://www.ncbi.nlm.nih.gov/pubmed/8808147.
[36] Liang S, Pan J. An endogenous dopaminergic tone acting on dopamine D 3 receptors may be involved in diurnal changes of tuberoinfundibular dopaminergic neuron activity and prolactin secretion in estrogen-primed ovariectomized rats. Brain Res. Bull. [Internet]. 2012;87:334–339. Available from: http://dx.doi.org/10.1016/j.brainresbull.2011.11.018.
[37] Liang S, Hsu S, Pan J. Involvement of dopamine D 2 receptor in the diurnal changes of tuberoinfundibular dopaminergic neuron activity and prolactin secretion in female rats. J. Biomed. Sci. 2014;21:1–9.
[38] Gudelsky GA, Nansel DD, Porter JC. Role of Estrogen in the Dopaminergic Control of Prolactin Secretion. Endocrinology. 1981;108:440–444.
[39] Morel GR, Carónc RW, Cónsoleb GM, et al. Estrogen inhibits tuberoinfundibular dopaminergic neurons but does not cause irreversible damage. Brain Res. Bull. 2009;80:347–352.
[40] Foord SM, Peters JR, Dieguez C, et al. Thyrotropin Regulates Thyrotroph Responsiveness to Dopamine in Vitro. Endocrinology. 1986;118:1319–1326.
[41] Ishibashi M, Yamaji T. Direct effects of thyrotropin-releasing hormone, cyproheptadine, and dopamine on adrenocorticotropin secretion from human corticotroph adenoma cells in vitro. J. Clin. Invest. 1981;68:1018–1027.
[42] Ishibashi M, Yamaji T. Direct effects of catecholamines, thyrotropin-releasing hormone, and somatostatin on growth hormone and prolactin secretion from adenomatous and nonadenomatous human pituitary cells in culture. J. Clin. Invest. 1984;73:66–78.

[43] Dumas EO, Pollack GM. Opioid Tolerance Development: A Pharmacokinetic/Pharmacodynamic Perspective. AAPS J. [Internet]. 2008;10:537–551. Available from: http://www.springerlink.com/index/10.1208/s12248-008-9056-1.

[44] Cho D, Zheng M, Min C, et al. Phosphorylation Mediate Resensitization of Dopamine D 2 Receptors. 2010;24:574–586.

[45] Adachi K, Hasegawa M, Fujita S, et al. Prefrontal, accumbal [shell] and ventral striatal mechanisms in jaw movements and non-cyclase-coupled dopamine D1-like receptors. Eur. J. Pharmacol. 2003;473:47–54.

[46] Gao W, Lee TH, Ph D, et al. Alterations in Baseline Activity and Quinpirole Sensitivity in Putative Dopamine Neurons in the Substantia Nigra and Ventral Tegmental Area after Withdrawal from Cocaine Pretreatment. Neuropsychopharmacology. 1998;18:222–232.

[47] Li H, Yan Z. Analysis of amino acid neurotransmitters in hypothalamus of rats during cerebral ischemia–reperfusion by microdialysis and capillary electrophoresis. Biomed. Chromatogr. 2010;24:1185–1192.

[48] Granveau-Renouf S, Valente D, Durocher A, et al. Microdialysis study of bromocriptine and its metabolites in rat pituitary and striatum. Eur. J. Drug Metab. Pharmacokinet. 2000;25:79–84.

Supplementary Table I. Parameter estimates for ACTH, PRL and TSH with and without covariate effect

		Without covariate effect	With covariate effect
ACTH			
OFV		-31.3	-117.3
$Baseline_{DAY1}$ (pg/ml)		3.74 (17%)	2.80 (19%)
$Baseline_{DAY8}$ (pg/ml)		3.74 (17%)	2.80 (19%) * 1.85 (37%)
	$IIV_{Baseline}$	0.68 (71%) [0%]	0.71 (67%) [0%]
Slope ($[ng/ml]^{-1}$)		0.87 (43%)	0.79 (45%)
K_{DEG} (min^{-1})		0.0146 (24%)	0.0150 (22%)
$K_{REL,DAY1}$ (min^{-1})		0.00760 (29%)	0.0055 (30%)
$K_{REL,DAY8}$ (min^{-1})		0.00760 (29%)	0.0055 (30%) * (1 + 2.1 (41%) * dose)[a]
	RUV	0.27 (21%) [3%]	0.22 (16%) [3%]
PRL			
OFV		373.5	290.9
$Baseline_{DAY1}$ (pg/ml)		262 (25%)	296 (38%)
$Baseline_{DAY8}$ (pg/ml)		262 (25%)	296 (38%) * (1 + 0.34 * dose)[a]
	$IIV_{Baseline}$	0.67 (28%) [4%]	0.69 (28%) [2%]
$Extent_{Plac,DAY1}$ (pg/ml)		8.72 (fix)	8.72 (fix)
$Extent_{Plac,DAY8}$ (pg/ml)		8.72 (fix)	8.72 (fix) * 0.34 (11%)
$K_{IN,\ Plac}$ (min^{-1})		1.65 (fix)	1.65 (fix)
$K_{DEC,\ Plac}$ (min^{-1})		1.55 (fix)	1.55 (fix)
E_{MAX}		-0.959 (13%)	-0.963 (11%)
EC_{50} (ng/ml)		0.933 (99%)	0.556 (174%)
K_{DEG} (min^{-1})		0.0652 (22%)	0.068 (5.9%)
	RUV	0.79 (18%) [3%]	0.63 (18%) [3%]
TSH			
OFV		-270.0	-362.1
$Baseline_{DAY1}$ (pg/ml)		293 (4.7%)	384 (7.0%)
$Baseline_{DAY8}$ (pg/ml)		293 (4.7%)	384 (7.0%) * 0.61 (21%)
	$IIV_{Baseline}$	0.045 (30%) [9%]	0.071 (27%) [4%]
$K_{DEC,\ Plac}$ (min^{-1})		0.00489 (fix)	0.00489 (fix)
E_{MAX}		-0.794 (32%)	-0.948 (149%)
$EC_{50,DAY1}$ (ng/ml)		178 (34%)	27.1 (26%)
$EC_{50,DAY8}$ (ng/ml)		178 (34%)	27.1 (26%) * (1 + 2.84 (48%) * dose)[a]
K_{DEG} (min^{-1})		0.126 (20%)	0.070 (13.2%)
	RUV	0.18 (19%) [2%]	0.14 (17%) [3%]

[a] **dose in mg/kg**

ACTH: adenocorticotropic hormone; ECF: extracellular fluid; EC_{50}: concentration at half maximal drug effect; E_{MAX}: maximal drug effect; GH: growth hormone; k_{DEC}: dose-independent hormone decay; k_{DEG}: hormone elimination rate; k_{REL}: hormone release reate; OFV: objective function value; PRL: prolactin; RSE: relative standard error; RUV: residual unexplained variability; S_0: E_{MAX}/EC_{50}; TSH: thyroid stimulating hormone

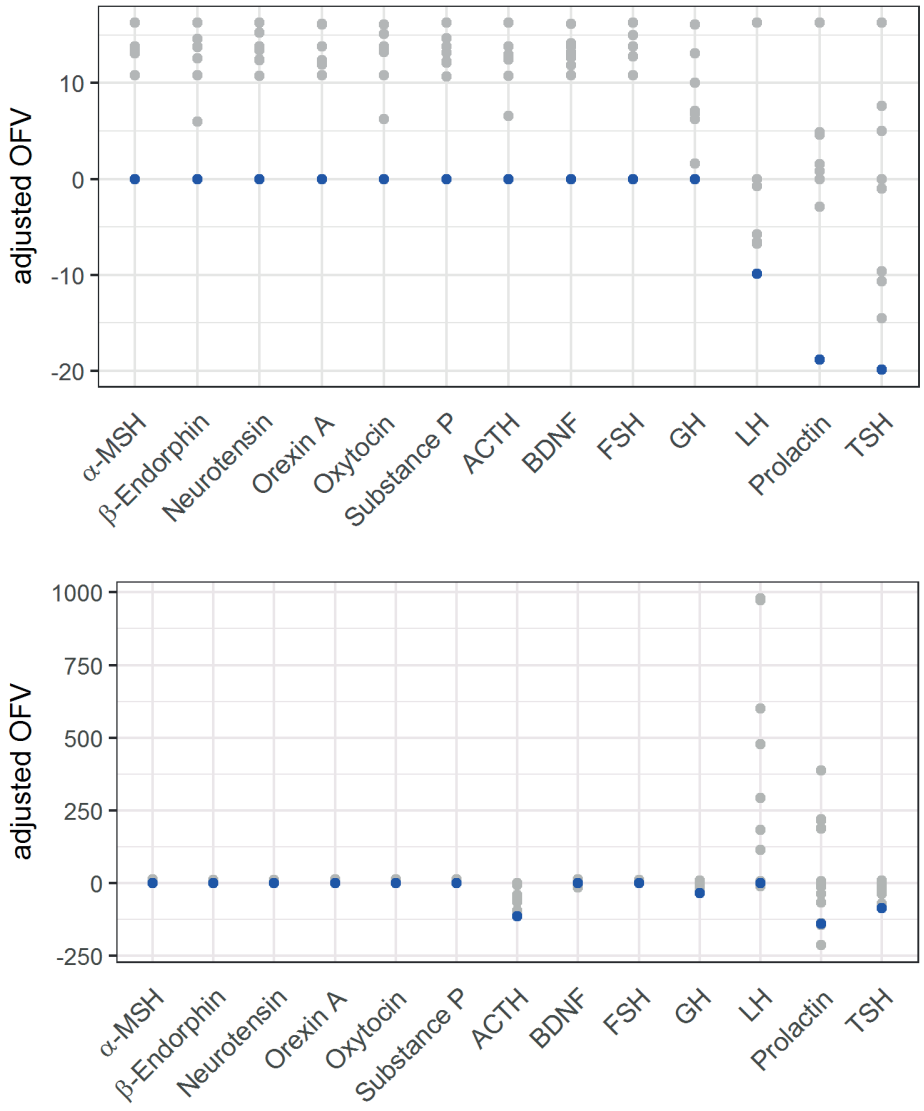

Supplementary Figure 1. Visualization of the automated model selections for the baseline model (A) and the PK/PD model (B) on basis of adjusted objective function value (suppl. Equations part I, 8). Grey dots represent the adjusted objective function value for each evaluated model, while blue dots represent the selected models.

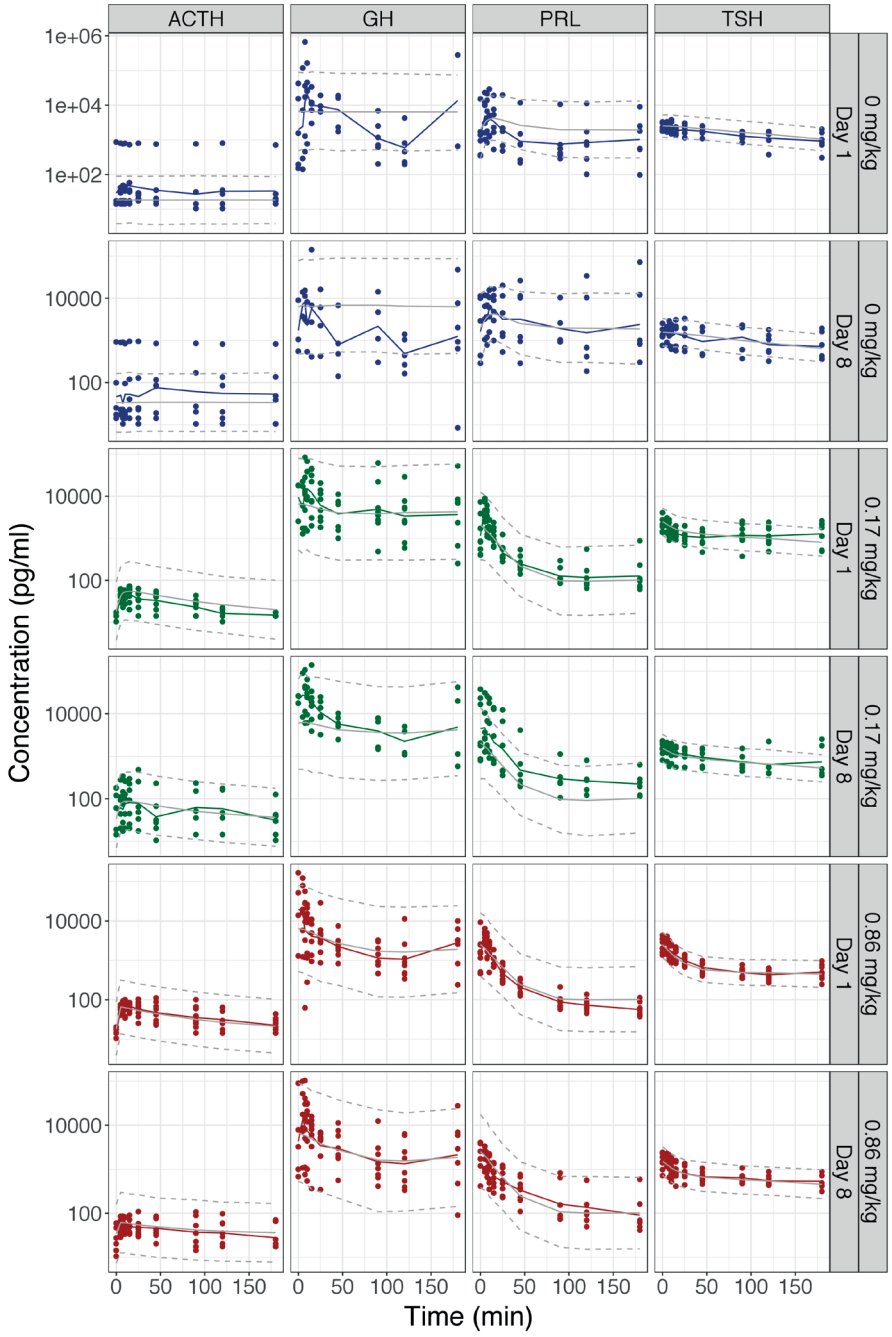

Supplementary Figure 2. Visual predictive check of the quinpirole PK/PD models for ACTH, GH, PRL and TSH at experiment day 1 and 8. The colored dots represent the observed data, with the solid colored lines showing the mean of the observations. The solid grey line shows the mean, and the dashed grey lines the 90% confidence interval of 500 simulations.

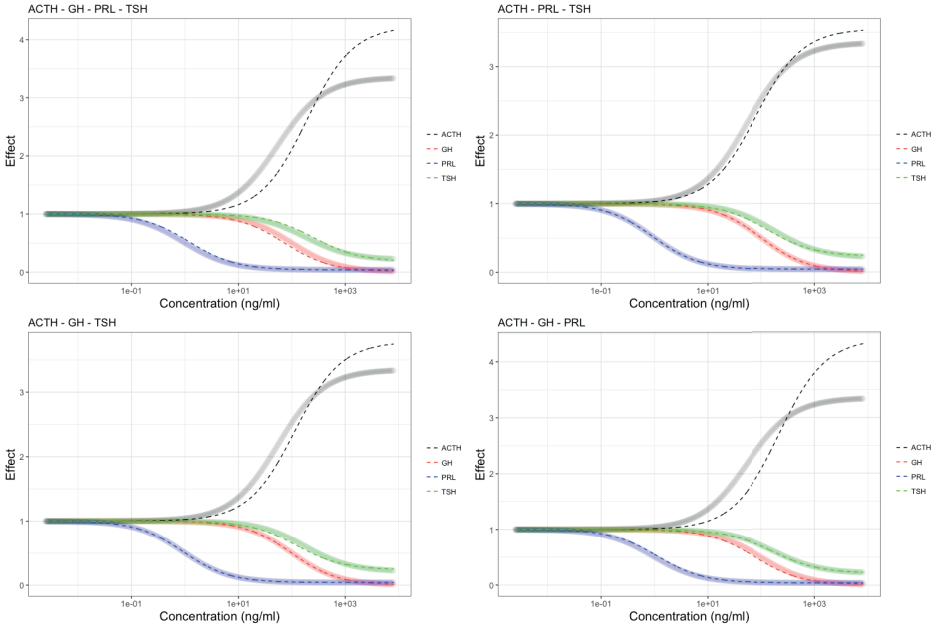

Supplementary Figure 3. A) Simulated concentration-effect relations for ACTH (black), TSH (green), GH (red) and PRL (blue) on basis of the parameter estimates in table III as compared to the fits by the operational model (equation 1). Each figure represents a different scenario with regard to the hormones included in the relation between tau and D_2 receptor expression (equation 2). The signal transduction efficiency τ is assumed dependent on pituitary D_2 receptor expression for the hormones indicated above each figure. For the hormone not included, the signal transduction efficiency τ is estimated separately.

Supplementary Equations

Inter-individual and residual variability

$$\vartheta_i = \vartheta_{pop} * e^{\eta i} \quad \text{(Eq. 1)}$$

$$Log(C_{obs\,,\,i\,,\,j}) = Log(C_{pred}\,,\,i\,,\,j) + \varepsilon_{i\,,\,j} \quad \text{(Eq. 2)}$$

$\boldsymbol{\vartheta_i}$ is the estimated parameter for individual i; $\boldsymbol{\vartheta_{pop}}$ is the estimated parameter for the population; $\boldsymbol{\eta_i}$ follows a normal distribution with mean 0 and variance ω^2; $\boldsymbol{C_{obs,i,j}}$ is the observed concentration data point for individual i at timepoint j; $\boldsymbol{C_{pred,i,j}}$ is the predicted concentration for data point for individual i at timepoint j; $\boldsymbol{\varepsilon_{i,j}}$ follows a normal distribution with mean 0 and variance σ^2.

Pharmacokinetic model

$$\frac{dA_{QP\,,\,PL}}{dt} = -\frac{CL_{PL\,,\,o}}{V_{PL}} * A_{QP\,,\,PL} - \frac{CL_{PL\,,\,ECF}}{V_{PL}} * A_{QP\,,\,PL} + \frac{CL_{ECF\,,\,PL}}{V_{ECF}} * A_{QP\,,\,ECF} \quad \text{(Eq. 3a)}$$

$$\frac{dA_{QP\,,\,ECF}}{dt} = \frac{CL_{PL\,,\,ECF}}{V_{PL}} * A_{QP\,,\,PL} - \frac{CL_{ECF\,,\,PL}}{V_{ECF}} * A_{QP\,,\,ECF} \quad \text{(Eq. 3b)}$$

With $A_{QP\,,\,PL\,,\,0} = Dose\,,\quad A_{QP\,,\,ECF\,,\,0} = 0$

Where $C_{QP\,,\,PL} = \frac{A_{QP\,,\,PL}}{V_{PL}}\,,\quad C_{QP\,,\,ECF} = \frac{A_{QP\,,\,ECF}}{V_{ECF}}$

$\boldsymbol{A_{QP,PL}}$ is the amount of quinpirole in plasma; $\boldsymbol{A_{QP,ECF}}$ is the amount of quinpirole in brain$_{ECF}$; $\boldsymbol{CL_{PL,o}}$ is the elimination clearance of quinpirole from plasma; $\boldsymbol{V_{PL}}$ is the volume of distribution of quinpirole in plasma; $\boldsymbol{CL_{PL,ECF}}$ is the clearance of quinpirole from plasma to brain$_{ECF}$; $\boldsymbol{CL_{ECF,PL}}$ is the clearance of quinpirole from brain$_{ECF}$ to plasma; $\boldsymbol{V_{ECF}}$ is the volume of distribution of quinpirole in brain$_{ECF}$; $\boldsymbol{C_{QP,PL}}$ is the concentration of quinpirole in plasma; $\boldsymbol{C_{QP,ECF}}$ is the concentration of quinpirole in plasma.

Baseline models

No pattern

$$C_{HORM\,,\,BSL} = BSL_{HORM} \quad \text{(Eq. 4)}$$

Circadian rhythm function

$$C_{HORM\,,\,BSL} = BSL_{HORM} + A * cos\left(\frac{2\pi}{p} * (time - \varphi)\right) \quad \text{(Eq. 5)}$$

Placebo Bateman function

$$C_{HORM\,,\,BSL} = BSL_{HORM} + \frac{D * k_e}{k_{DEC} - k_{IN}} * \left(e^{-kINtime} - e^{-kDECtime}\right) \quad \text{(Eq. 6)}$$

Placebo exponential decay function

$$C_{HORM\,,\,BSL} = BSL_{HORM} * e^{-\,kDECtime} \quad \text{(Eq. 7)}$$

$\boldsymbol{C_{HORM,BSL}}$ is the hormone concentration given no drug effect; $\boldsymbol{BSL_{HORM}}$ is the hormone concentration at baseline at time = 0; $\boldsymbol{A}$ is the amplitude; $\boldsymbol{p}$ is the period; $\boldsymbol{\varphi}$ is the phase shift; $\boldsymbol{D}$ determines the extent of the placebo response; $\boldsymbol{k_a}$ the rate at which the placebo response occurs; $\boldsymbol{k_e}$ the rate at which the placebo response disappears.

Objective function value

$$adjOFV = OFV_{test} - OFV_{ref} + inv.\chi^2\,(\,1 - p.value\,,\,df\,) \quad \text{(Eq. 8)}$$

adjOFV is the adjusted objective function value to compare two models. An adjOFV below 0 indicates a significant improvement of the test model over the reference model. The **inv. $\boldsymbol{\chi^2}$** is a statistical test to compare two models. For example, a significant improvement with a p-value of 0.05 and 1 degree of freedom is equivalent to a decrease of 3.84 points in OFV according to the χ^2-test.

Drug effect models

Slope model

$$E = 1 + slope * C_{QP} \quad \text{(Eq. 9)}$$

E_{MAX} model

$$E = 1 + \frac{E_{MAX} * C_{QP}}{EC_{50} + C_{QP}} \quad \text{(Eq. 10)}$$

Alternative E_{MAX} model

$$E = 1 + \frac{S_0 * E_{MAX} * C_{QP}}{E_{MAX} + S_0 * C_{QP}} \quad \text{(Eq. 11)}$$

On-off model

$$E = \begin{cases} 0\,, & \& \; C_{QP} = 0 \\ E_{MAX}\,, & \& \; C_{QP} > 0 \end{cases} \quad \text{(Eq. 12)}$$

$\boldsymbol{E}$ is the magnitude of drug effect; ***Slope*** is the parameter that determines the strength of the drug effect; $\boldsymbol{C_{QP}}$ is the drug concentration at the target site, either plasma or $brain_{ECF}$; $\boldsymbol{E_{MAX}}$ is the maximal effect; $\boldsymbol{EC_{50}}$ is the drug concentration at half maximal effect; $\boldsymbol{S_0}$ is defined as $\boldsymbol{E_{MAX}/EC_{50}}$.

Link models

No effect

$$C_{HORM\,,\,PL} = C_{HORM\,,\,BSL} \quad \text{(Eq. 13)}$$

Direct response model

$$C_{HORM,PL} = C_{HORM,BSL} * E \quad \text{(Eq. 14)}$$

Turnover model (effect on hormone release)

$$\frac{dC_{HORM,PL}}{dt} = k_{DEG} * C_{HORM,BSL} * E - k_{DEG} * C_{HORM,PL} \quad \text{(Eq. 15)}$$

Pool model (effect on hormone release)

$$\frac{dC_{HORM,Pool}}{dt} = k_{DEG} * C_{HORM,BSL} - k_{REL} * E * C_{HORM,Pool} \quad \text{(Eq. 16a)}$$

$$\frac{dC_{HORM,PL}}{dt} = k_{REL} * E * C_{HORM,Pool} - k_{DEG} * C_{HORM,PL} \quad \text{(Eq. 16b)}$$

$\boldsymbol{C_{HORM,PL}}$ is the hormone concentration in plasma; $\boldsymbol{k_{DEG}}$ is the hormone turnover rate; $\boldsymbol{k_{DEG} * C_{HORM,BSL}}$ is equivalent to $\boldsymbol{k_{IN}}$, the hormone production rate within the pool compartment; $\boldsymbol{C_{HORM,POOL}}$ is the hormone concentration in the pool; $\boldsymbol{k_{REL}}$ is the hormone release rate from the pool into plasma.

Covariate models

$$\vartheta_{DAY} = \vartheta_{pop} * (1 + COV) \quad \text{(Eq. 17)}$$

$$\vartheta_{DAY} = \vartheta_{pop} * (1 + COV_{SLP} * Dose) \quad \text{(Eq. 18)}$$

$$\vartheta_{DAY} = \vartheta_{pop} * (1 + \frac{COV_{MAX} * Dose}{COV_{50} + Dose}) \quad \text{(Eq. 19)}$$

$\boldsymbol{\vartheta_{DAY}}$ is the estimated parameter for the specific day; $\boldsymbol{\vartheta_{pop}}$ the population parameter; $\boldsymbol{COV}$ the dose independent covariate parameter; $\boldsymbol{COV_{SLP}}$ the dose dependent covariate parameter following a linear relation; $\boldsymbol{COV_{MAX}}$ and $\boldsymbol{COV_{50}}$ the dose dependent covariate parameters following a non-linear relation. The covariate effect is set to zero for day 1.

Supplementary Methods

Additional PK experiment as external validation of the quinpirole PK model

The experimental procedures applied in this additional experiment have been previously described (Wong et al. Eur J Pharm Sci. 2018:111;514-525), which involved similar procedures as those in the current manuscript with some modifications. In brief, 15 male Wistar rats were used, and 7 of which received microdialysis surgery in addition to the femoral artery and vein cannulations. Two microdialysis guides (CMA 12 Guide Cannula, Aurora Borealis Control BV, Schoonebeek, the Netherlands) were embedded in the brain striatum (AP − 1.0; L 3.2; V − 3.5 mm relative to bregma) and cerebellum (AP − 2.51; L 2.04; V

− 3.34 mm, at an angle of 25° from the dorsoventral axis (toward anterior) and 11° lateral from the anteroposterior axis relative to lambda). The rats were given 7 days to recover from surgery. One day before the experiment, the microdialysis guides were substituted by the microdialysis probes (CMA 12 Elite Polyarylethersulfone, 4 mm membrane, cut-off 20 kDA, Aurora Borealis Control BV, Schoonebeek, the Netherlands).

On the day of experiment, rats received an IV infusion of quinpirole 1 mg/kg at the start of experiment (t = 0 min). The duration of the infusion was either 10 min (for 12 rats) or 0.5 min (for 3 rats). Plasma and brain microdialysate were collected and analyzed in the same manner as in the current manuscript. The plasma and striatum ECF data were used to validate the PK model.